JOINT EUROPEAN TORUS JET

JET–P(93)23

H.J. de Blank, M.F.F. Nave, W. Kerner, G.T.A. Huysmans

Resistive Ballooning Analysis for Edge Localized Modes in JET Discharges

Resistive Ballooning Analysis for Edge Localized Modes in JET Discharges

H.J. de Blank, M.F.F. Nave[1], W. Kerner, G.T.A. Huysmans[2]

JET-Joint Undertaking, Culham Science Centre, OX14 3DB, Abingdon, UK

[1]Associaçao 1ST/EURATOM, Lisbon, and LNETI Sacavém, Portugal.
[2]FOM-Instituut voor Plasmafysica 'Rijnhuizen', Nieuwegein, the Netherlands.

April 1993

RESISTIVE BALLOONING ANALYSIS FOR EDGE LOCALIZED MODES IN JET DISCHARGES

H.J. de Blank, M.F.F. Nave[1], W. Kerner, and G.T.A. Huysmans[2]

JET Joint Undertaking, Abingdon, Oxon, OX14 3EA, UK.

[1] *Associação IST/EURATOM, Lisbon, and LNETI Sacavém, Portugal*

[2] *FOM-Instituut voor Plasmafysica 'Rijnhuizen', Nieuwegein, the Netherlands*

Introduction

Edge localized modes (ELMs) are observed during H-mode discharges in JET with widely varying amplitudes and repetition rates [1,2,3]. They can be small and very frequent ('grassy') when an H-mode builds up, but as the edge electron temperature increases, they become larger and much less frequent. The larger, 'singular' ELMs, which were discussed in Ref. [3], are similar to the 'type III' ELMs in DIII-D [4] and ASDEX [5]. Prior to these singular ELMs in JET, pressure gradients near the edge plasma are found to be well below the ideal ballooning stability limit, while resistive ballooning modes with medium to large toroidal mode numbers, $n \geq 10$, are unstable.

In the first part of this paper we extend this analysis to the fast events which sometimes terminate high-β_p or hot-ion phases in JET discharges, varying from large ELMs to global events in which central $m = 1$ activity and fast edge losses occur simultaneously. We find that prior to some of these events, edge pressure gradients are much closer to the ideal ballooning limit, and that the relative importance of the pressure gradient and of resistivity for stability of the plasma near the edge varies from case to case.

In part two of the paper, we present asymptotic solutions of the ballooning equation obtained from a generalization of the two-scale expansion method of Ref. [6] to flux surfaces with finite aspect ratio. The result makes an efficient computation of the ballooning Δ' near the JET plasma edge possible, taking into account up-down asymmetry.

Phenomenology

ELMs are primarily observed as a sharp rise in the D_α signal. During an ELM a short (200μs) broad-band (0–120 kHz) burst of magnetic fluctuations and density fluctuations are observed. Smaller, but otherwise similar, fluctuation bursts which do not give rise to a D_α peak often occur as well. The ELMs and smaller turbulent

events occur with irregular intervals and amplitudes, though larger ELMs tend to suppress the activity for some time afterwards. This pattern of ELMs preceded by smaller bursts suggests a cascade of particle and energy losses by a locally increased pressure gradient. Alternatively, ELMs can be triggered by enhanced impurity influx, gas puff, or a heat pulse from a sawtooth or fishbone instability arriving at the edge. This indicates that a locally increased pressure gradient and increased resistivity can both trigger an ELM. We conclude that the ELM is caused by a resistive MHD mode.

Clues for the underlying instability come from the observation of precursor oscillations in the edge which usually start several milliseconds before the ELM (see ref. [2]) :

- The precursor frequency is typically 50–100 kHz. In some cases the frequency changes just before the ELM (Fig. 1a), in other cases the frequency is constant throughout the event (Fig. 1b).
- The phase differences between two coils indicate toroidal mode numbers n=8–15, suggesting a ballooning type instability.
- Density fluctuations are detected at several positions in the plasma with a multichannel microwave reflectometer. The precursor density fluctuations appear to be localized several centimeters inside the separatrix, while the turbulent phase extends further outward.

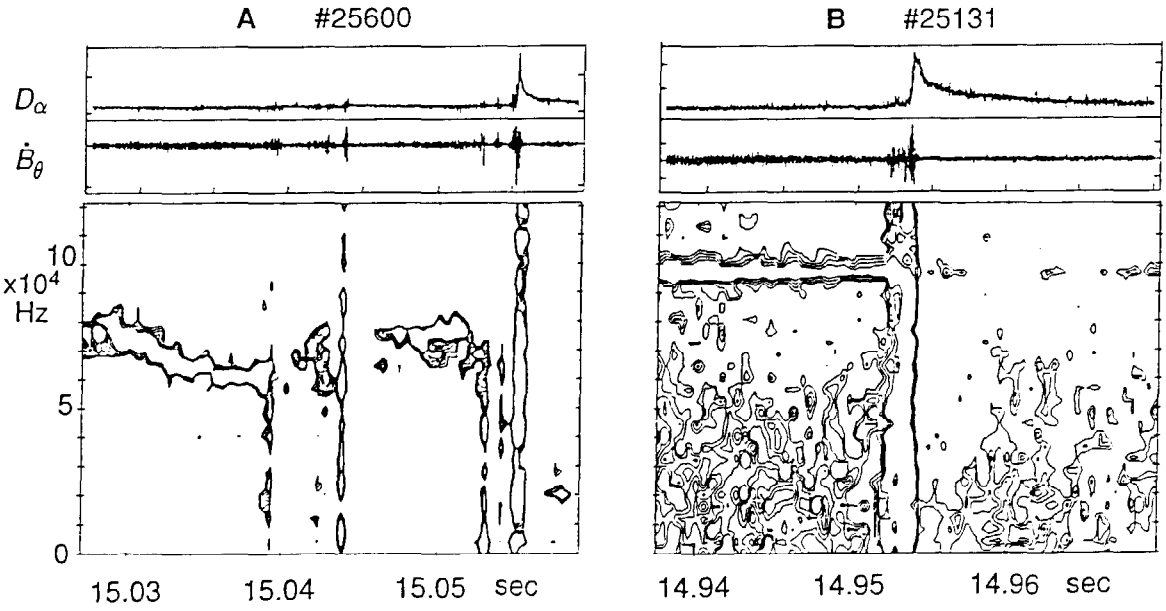

Fig. 1 *$\dot{B}_\theta$ frequency spectrum versus time from fast magnetic coils in two JET H-modes. Also shown are D_α signals which indicate particle losses from the edge.*
1A. *Long-lived coherent oscillations with frequencies~80 kHz are visible, changing in frequency shortly before the ELMs, which are visible as broad band events. Some smaller turbulent bursts, not visible on the D_α signal, precede the ELMs.*
1B. *A similar precursor (100 kHz) is visible with a frequency not affected by the ELM at all, even after the turbulent event, when the mode amplitude is much reduced.*

Because these precursors can exist long before an ELM occurs and are not growing shortly before the onset of turbulence, their effect is probably to change the equilibrium, building up larger gradients near the edge. Subsequently, turbulence sets in quickly at a broad range of frequencies. Exponential growth of a monochromatic precursor, as clearly seen in ASDEX [5], is visible in JET for at most a few cycles and often not at all.

1 Resistive ballooning stability

For a number of discharges we have analyzed the stability of resistive ballooning modes at 3–10 cm inside the plasma edge (usually the separatrix of a double-null X-point configuration). The equilibria were reconstructed from the magnetic and profile data with the IDENTD code [7]. The full equilibrium shape and the measured edge pressure and current density gradients are fed into the ideal MHD ballooning stability code HBT[8]. The edge pressure gradients are given by the following profiles,

- T_e and n_e from LIDAR Thomson scattering,
- n_e from the microwave reflectometer and the far infrared interferometer,
- T_i, Z_{eff} from charge exchange spectroscopy.

The uncertainty in dp/dr (almost 100% over 5 cm) is sufficiently small for the present discussion. HBT recomputes the equilibrium and performs a full ideal MHD ballooning stability analysis using either the Suydam method[9] or direct integration of the ballooning equation.

Subsequently, we obtain Δ' from the ballooning equation $d^2\xi/d\theta^2 = V(\theta)\xi$ in the limit of high shear by assuming a square well potential $V(\theta)$, with depth and width chosen to give the correct values of $\int_{-\infty}^{\infty} V(\theta)\,d\theta$ and the HBT ideal stability limit α_{crit}. Figure 2 shows the resulting $\Delta'(\alpha)$ for several discharges, together with points representing the resistive Δ values for $n = 5$ and $n = 10$ in these cases.

The resistive ballooning stability is determined by matching the ideal MHD Δ' to the compressible resistive layer solution, taken from the model of Drake and Antonsen [10].

In Fig. 3, the data shown in Fig. 2 is presented for $n = 10$, highlighting the distances to the ideal and the resistive stability boundaries. Case *(i)* is a hot-ion H-mode with high beryllium influx ($Z_{\mathrm{eff}} = 3.5$ near the edge) just before a large ELM. The ideal ballooning limit is found to be considerably above the observed pressure gradient and comes closest to it ($\sim 3dp/dr$) at $r/a = 0.95$. Only resistive ballooning instabilities with mode numbers $n \geq 8$ are unstable. In case *(ii)*, a H-mode discharge suffers a 'carbon bloom'. A fast collapse does not take place. The figure shows that the plasma edge is far from both stability limits. Case *(iii)* is a high-β_{p} hot-ion discharge just before a high-performance terminating event. The

ideal ballooning limit is approached near the plasma edge. Case *(iv)* is similar, but is found to be somewhat closer to resistive instability. Finally, in case *(v)* a sawtooth and two ELMs occur within 1 ms, though we find that the edge is ballooning stable. A possible explanation is that the energy released by the central $m = 1$ instability affects the edge stability.

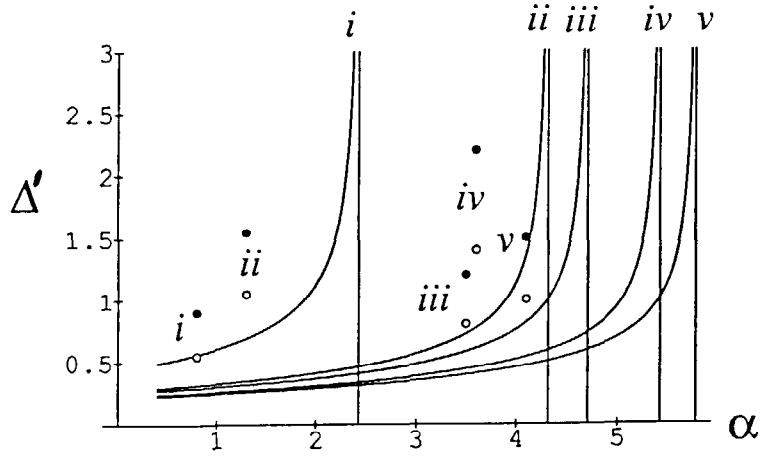

Fig. 2 *Δ-values from ideal and resistive ballooning theory versus* $\alpha = -2\mu_0(dp/dr)r^2/RB_\theta^2$ *for several hot ion modes in JET, prior to enhanced edge losses. The following events are shown,*

i) discharge 27793, before large singular ELM. The magnetic shear $s = 4.0$,
ii) discharge 25865, before carbon bloom, $s = 6.4$,
iii) discharge 26095, high-β_p *terminating event,* $s = 6.9$,
iv) discharge 26087, as (iii), $s = 7.7$,
v) discharge 26788, high-β_p*, before carbon bloom,* $s = 8.2$.

For each event, the figure shows a:

- *curved line: ideal MHD* Δ' *versus* α *for fixed shear* s.
- *vertical line: ideal stability boundary* $\alpha = \alpha_{\text{crit}}$ *from HBT.*
- *solid circle: resistive layer* Δ *for* $n = 5$
- *open circle: idem, for toroidal mode number* $n = 10$

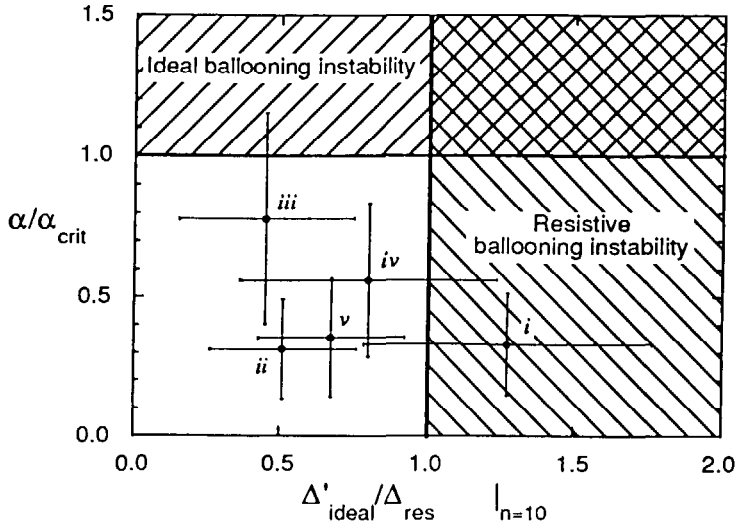

Fig. 3 *Ideal and resistive ballooning stability diagram, showing the five cases presented in Fig. 2. The pressure gradient (vertical axis) is normalized to the ideal ballooning limit. The resistive layer Δ is normalized to the ideal Δ'. Type III-ELMs like (i) can be found near the resistive boundary for $n = 10$, while the high-β_p cases (iii, iv) are closer to the ideal limit.*

2 Improved computation of the ideal ballooning Δ'

For the present discussion we write the ballooning equation [11] in operator form, $HF(\theta) = 0$, where marginal stability is given by $F \to 0$ when the generalized poloidal coordinate $\theta \to \pm\infty$. Since the marginally stable solution $F(\theta)$ can be a very broad function while the ballooning operator H is dominated by oscillating terms, it is advantageous to limit numerical integration by matching the numerical solution to an analytic asymptotic expansion valid for large θ. This technique, which exploits a two-scale expansion by separating periodic and polynomial terms in θ, has been presented and used in Ref. [9] in the approximation of large aspect ratio of the torus.

Here, we generalize the two-scale expansion to finite aspect ratio, in order to apply it to the JET plasma edge. We introduce some compact notation and write the ballooning operator as

$$H = \frac{d}{d\theta}\Big[\Big(\frac{1}{JR^2B_\theta^2} + \frac{P^2}{t}\Big)\frac{d}{d\theta}\Big] + \Big(c + \frac{d\tilde{g}}{d\theta}P\Big)\,, \qquad (1)$$

containing the shear integral $P(\theta) = \int_{\theta_0}^{\theta} s(\theta)\,d\theta$ and the periodic functions

$$s = \frac{\partial}{\partial\psi}\Big(\frac{IJ}{R^2}\Big)\,, \qquad t = \frac{JB^2}{R^2B_\theta^2}\,, \qquad c = 2\frac{Jp'}{B^2}\frac{\partial}{\partial\psi}(p + \tfrac{1}{2}B^2)\,, \qquad g = \frac{Ip'}{B^2}\,,$$

where J is the Jacobian of the coordinates (ψ, θ, ϕ), and $I(\psi) = RB_\phi$. Introducing the notation

$$\overline{X} \equiv \frac{1}{2\pi}\oint X\,d\theta\,, \qquad \tilde{X} \equiv X - \overline{X}\,, \qquad \widetilde{\int}(X) \equiv \int^{\theta}\tilde{X}\,d\theta\,,$$

the polynomial and oscillating parts in the shear integral can be separated: $P(\theta) = \overline{s}(\theta - \theta_1) + \widetilde{f}(s)$, with $\theta_1 \equiv \theta_0 - \overline{\int_{\theta_0}^{\theta} \tilde{s}\, d\theta'}/\overline{s}$.

Consequently, for large $|\theta|$ the function $F(\theta)$ can be expanded in powers of $(1/\theta)$ as follows,

$$F = \sum_{k\geq 0} \theta^{\lambda-k} f_k(\theta) = \theta^{\lambda}\Big[f_0(\theta) + \frac{f_1(\theta)}{\theta} + \frac{f_2(\theta)}{\theta^2} + O(\frac{1}{\theta^3})\Big]\,, \tag{2}$$

where the functions $f_k(\theta)$ can be restricted to periodic functions in θ. Substituting expressions (1) and (2) in the ballooning equation and evaluating the derivatives of $\theta^{\lambda-k}$, it is found that the expansion of the operator H in $(1/\theta)$ consists of just five terms, $HF = \sum_{i=0}^{4}\sum_{k\geq 0} H_{i,k} f_k \theta^{\lambda-i-k}$. These terms are

$$\begin{aligned}
H_{0,k} &= \overline{s}^2 D\frac{1}{t}D\,,\\
H_{1,k} &= (\lambda-k)\overline{s}^2 D\frac{1}{t} + (\lambda-k+2)\frac{\overline{s}^2}{t}D + 2\overline{s}D\frac{P_1}{t}D + D\tilde{g}\overline{s} - \tilde{g}\overline{s}D\,,\\
H_{2,k} &= (\lambda-k)(\lambda-k+1)\frac{\overline{s}^2}{t} + 2(\lambda-k)D\frac{P_1}{t} + 2(\lambda-k+1)\overline{s}\frac{P_1}{t}D +\\
&\qquad DaD - P_1\tilde{g}D + D\tilde{g}P_1 + c - \tilde{g}\tilde{s}\,,\\
H_{3,k} &= 2\overline{s}(\lambda-k)\frac{P_1}{t} + (\lambda-k)Da + (\lambda-k)aD\,,\\
H_{4,k} &= (\lambda-k)(\lambda-k-1)a\,,
\end{aligned}$$

where

$$D \equiv \frac{d}{d\theta}, \qquad P_1 \equiv \widetilde{f}(s) - \overline{s}\theta_1, \qquad a \equiv \frac{1}{JR^2B_\theta^2} + \frac{P_1^2}{t}\,.$$

Subsequently, we solve the ballooning equation order by order. The leading order equation is just $f_0(\theta) =$ constant. The next order in $(1/\theta)$ yields $\overline{s}f_1/f_0 = (\lambda\overline{s} + \overline{gt})\widetilde{f}(t)/\overline{t} - \widetilde{f}(gt)+$ an integration constant. The average part of the $O(1/\theta^2)$ equation determines the Mercier index λ, while the oscillating part is an expression for Df_2. This expression is then substituted in the averaged $O(1/\theta^3)$ equation in order to determine the integration constant in f_1. The resulting general solution is given by

$$\begin{aligned}
F &= f_0\big[F(\lambda_+) + \Delta' F(\lambda_-)\big]\,,\\
F(\lambda) &= \theta^{\lambda}\Big[1 + \frac{f_1(\lambda,\theta)}{\theta} + O(\frac{1}{\theta^2})\Big]\,,\\
\overline{s}f_1(\lambda,\theta) &= \frac{\lambda\overline{s}+\overline{gt}}{\overline{t}}\widetilde{f}(t) - \widetilde{f}(gt) - \lambda\overline{s}\theta_1 + \frac{\lambda}{\overline{t}}\big\langle(gt-s)\widetilde{f}(t)\big\rangle + \frac{1}{\lambda\overline{t}}\big\langle D_M\widetilde{f}(t\overline{gt} - \overline{t}gt)\big\rangle\,,\\
\lambda_\pm &= -\tfrac{1}{2} \pm \sqrt{\tfrac{1}{4} + \overline{D_M}}\,,\\
D_M(\theta) &= \frac{\overline{t}}{\overline{s}^2}\Big[c - sg + g^2 t + (s-gt)\frac{\overline{gt}}{\overline{t}}\Big]\,.
\end{aligned}$$

section, involving the poloidal field strength $B_\theta(\theta)$, the curvature radius of the cross section $R_{\rm curv}(\theta)$, the minor radius of the flux surface r_0, and the major radius R_0. Defining

$$C_0 = \frac{J}{R^2}\,, \qquad C_3 = \frac{J}{R^2}\frac{R_0^2 B_\theta(0)}{R_{\rm curv} R B_\theta}\,,$$

$$C_1 = \frac{J}{R^2}\left(\frac{B_\theta(0) R_0}{B_\theta R}\right)^2, \qquad C_4 = C_3 \frac{R^2 - R_0^2}{2 r_0 R_0}\,,$$

$$C_2 = C_1 \frac{R^2 - R_0^2}{2 r_0 R_0}\,, \qquad C_5 = \frac{R_0^2 B_\theta(0)}{B_\theta^2 R^4}\frac{\partial Z}{\partial \theta}\,,$$

the Mercier index can be written as

$$\overline{D_M} = \frac{\alpha}{s^2}\left[\overline{C}_1(2\overline{C}_4 - \overline{C}_5) - 2\overline{C}_2(\overline{C}_3 + \overline{C}_5\epsilon_0) + \frac{R_0^2 B_\theta^2(0)}{I^2}(2\overline{C}_4 + \overline{C}_3/\epsilon_0)\right],$$

in agreement with known results. The expression for $f_1(\theta)$ is a new result, however. In terms of the coefficients C_i, f_1 contains three oscillating integrals, $\widetilde{J}(C_{0-2})$, and nine combinations $M_{0,1}$, $M_{0,2}$, $M_{1,2}$, and $M_{0-2,3-5}$, which are double double integrals over the cross section,

$$M_{i,j} = -M_{j,i} \equiv \overline{C_i \widetilde{J}(C_j)}\,.$$

A problem with the expressions for f_1 is that they diverge when $\overline{D_M}$ and λ_+ vanish, for instance in the limit of the $s - \alpha$ model. The method used in Ref. [10] to remove a similar divergence, is also applicable to the finite-ϵ case presented here.

Conclusions

We find that the edge pressure gradient remains well below the ideal ballooning limit before medium sized ELMs, and that resistive instability requires $n > 10$. However, in high-$\beta_{\rm p}$ and hot ion discharges the plasma edge can be very close to the ideal ballooning limit before an ELM or global event.

Resistive ballooning modes match the observations of long lived ELM precursors in JET. These precursors may cause the pressure gradient to build up closer to the separatrix. The sudden onset of broad band fluctuations in the ELM must be caused by a faster instability, possibly closer to the edge. The results in Ref. [3] suggest that the outer flux surfaces are then destroyed by a global resistive free boundary mode, driven by the edge current and pressure gradient. Thus, the combined action of these two types of resistive instabilities can explain the observed outflow of particles and energy.

The two-scale analysis in Ref. [6] is extended to finite aspect ratio. Using the resulting asymptotic expression for the eigenfunction, the ideal Δ' can be computed

without integrating the ballooning equation to very high values of $|\theta|$. The method is valid for up-down asymmetric flux surfaces and near a magnetic separatrix.

As in Ref. [6], for up-down asymmetric configurations some terms in the expressions for $F(\theta)$ require rearranging in order to avoid divergences when the Mercier index $\overline{D_M}$ vanishes.

Acknowledgement We thank W.P. Zwingmann for the IDENTD equilibrium reconstructions, G.J. Kramer and A.C.C. Sips for providing the reflectometer data, S. Ali-Arshad for magnetic fluctuations data, and H.R. Wilson for valuable discussions about the two-scale expansion and its application to the computation of Δ'.

References

[1] W. Kerner *et al.*, Bull. Am. Phys. Soc. **36** (1991) 2R13, p. 2310.

[2] S. Ali-Arshad *et al.*, Proceedings of the 19$^{\text{th}}$ European Conf. on Controlled Fusion and Plasma Physics, Innsbruck, Vol. I (1992) p. 227.

[3] G.T.A. Huysmans *et al.*, Proceedings of the 19$^{\text{th}}$ European Conf. on Controlled Fusion and Plasma Physics, Innsbruck, Vol. I (1992) p. 247.

[4] E. Doyle *et al.*, Proceedings of the 18$^{\text{th}}$ European Conf. on Controlled Fusion and Plasma Physics, Berlin, Vol. I (1991) p. 285.

[5] H. Zohm *et al.*, Nucl. Fusion **32** (1992) 489.

[6] H.R. Wilson, Plasma Phys. Contr. Fusion **6** (1990) 443.

[7] J. Blum *et al.*, Nucl. Fusion **30** (1990) 1475.

[8] J.P. Goedbloed *et al.*, 10$^{\text{th}}$ Int. Conf. on Plasma Physics and Controlled Nuclear Fusion Research, London, 1984 (IAEA, Vienna,1985) Vol. II, p. 165.
G.T.A. Huysmans *et al.*, (1990), Rijnhuizen Report 90-194, Nieuwegein, Netherlands.

[9] R.M.O. Galvão and J. Rem, Comp. Phys. Commun. **27** (1981) 399.

[10] J.F. Drake, T.M. Antonsen, Jr., Phys. Fluids **28** (1985) 544.

[11] J.W. Connor, R.J. Hastie, J.B. Taylor, Proc. R. Soc. **A365** (1979) 1.